Journal of Inorganic Biochemistry 107 (2012) 96–103

Contents lists available at SciVerse ScienceDirect

Journal of Inorganic Biochemistry

journal homepage: www.elsevier.com/locate/jinorgbio

The Fe(III) and Ga(III) coordination chemistry of 3-(1-hydroxymethylidene) and 3-(1-hydroxydecylidene)-5-(2-hydroxyethyl)pyrrolidine-2,4-dione: Novel tetramic acid degradation products of homoserine lactone bacterial quorum sensing molecules

Ariel A. Romano [a], Tobias Hahn [a], Nicole Davis [a], Colin A. Lowery [b], Anjali K. Struss [b], Kim D. Janda [b], Lars H. Böttger [c], Berthold F. Matzanke [c], Carl J. Carrano [a,*]

[a] Department of Chemistry and Biochemistry, San Diego State University, San Diego, CA 92182-1030, United States
[b] The Skaggs Institute for Chemical Biology and Departments of Chemistry and Immunology & Microbial Science, The Scripps Research Institute, Worm Institute for Research and Medicine (WIRM), The Scripps Research Institute, La Jolla, CA 92037, United States
[c] Isotopen Laboratorium, Sektion Naturwissenschaften, Universität zu Lübeck, Lübeck D-23528, Germany

ARTICLE INFO

Article history:
Received 28 July 2011
Received in revised form 14 October 2011
Accepted 20 October 2011
Available online 29 October 2011

Keywords:
Quorum sensing
Tetramic acid
Iron binding
Mössbauer spectroscopy

ABSTRACT

Bacteria use small diffusible molecules to exchange information in a process called quorum sensing (QS). An important class of quorum sensing molecules used by Gram-negative bacteria is the family of *N*-acylhomoserine lactones (HSL). It was recently discovered that a degradation product of the QS molecule 3-oxo-C_{12}-homoserine lactone, the tetramic acid 3-(1-hydroxydecylidene)-5-(2-hydroxyethyl)pyrrolidine-2,4-dione, is a potent antibacterial agent, thus implying roles for QS outside of simply communication. Because these tetramic acids also appear to bind iron with appreciable affinity it was suggested that metal binding might contribute to their biological activity. Here, using a variety of spectroscopic tools, we describe the coordination chemistry of both the methylidene and decylidene tetramic acid derivatives with Fe(III) and Ga(III) and discuss the potential biological significance of such metal binding.

1. Introduction

The ability of a population of unicellular bacteria to communicate with one another has enabled bacterial populations to act in a manner similar to multicellular organisms. This process, known as quorum sensing (QS), is mediated by the intercellular exchange of small, diffusible chemical signals called autoinducers [1–4]. These chemical signals have traditionally been classified according to structural similarities and the Gram classification of bacteria that respond to them. For example, Gram negative bacteria use *N*-acylhomoserine lactones (AHLs), whereas Gram-positive bacteria produce and respond to oligopeptides. As bacterial population density increases, the concentration of these autoinducers increases accordingly. Thus, upon reaching a threshold autoinducer concentration, bacteria coordinate gene expression and behave as a unified group. While this phenomenon is beneficial for the bacterial population, it often comes at the expense of human well-being, as QS regulates such processes as iron uptake, swarming, biofilm formation, and the production of virulence factors [5–7].

AHL-mediated QS is particularly important in the pathogenesis of the important human pathogen *Pseudomonas aeruginosa*, which possess a complex QS system. Two AHLs, *N*-3-oxododecaonyl homoserine lactone (3-oxo-C_{12}-HSL) and *N*-butrylhomoserine lactone (C_4-HSL), Fig. 1, play significant roles in the QS of *P. aeruginosa* [3]. The action of these signals regulates genes responsible for encoding enzymes such as elastases A and B, catalase, and superoxide dismutase as well as controlling biofilm formation and the production of other virulence factors [8]. *P. aeruginosa* is an opportunistic pathogen in humans, and is the most common Gram-negative bacterium associated with hospital-acquired infections [9]. Particularly notorious is the role of *P. aeruginosa* in infections of the lungs of cystic fibrosis patients, where lung defense systems are severely impaired [10]. After initial lung colonization, *P. aeruginosa* forms biofilms and, once formed, these biofilms are rarely cleared from the lungs of CF patients and the patients often succumb to the infection [11]. *P. aeruginosa* infections are also problematic in immunocompromised patients suffering from diseases such as AIDS and neurotropic cancer, as well as burn victims [12–14]. Regrettably, the increasing prevalence of antibiotic resistance in *P. aeruginosa* further exacerbates these problems [15].

Emerging research has demonstrated that QS not only assists *P. aeruginosa* in establishing infections by allowing for communication, but the QS signals themselves exert deleterious effects on

* Corresponding author. Tel.: +1 619 594 5929; fax: +1 619 594 4634.
E-mail address: carrano@sciences.sdsu.edu (C.J. Carrano).

0162-0134/$ – see front matter © 2011 Elsevier Inc. All rights reserved.
doi:10.1016/j.jinorgbio.2011.10.009

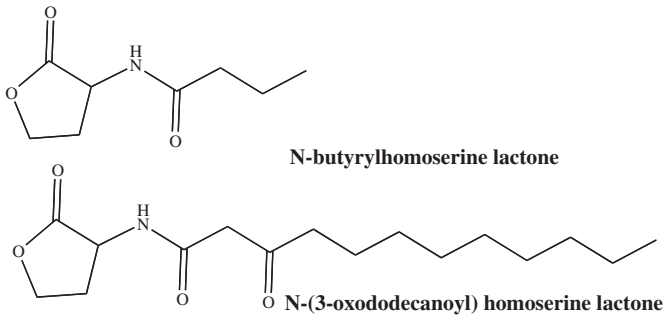

Fig. 1. Structures of two acylhomoserine lactone QS signals employed by *P. aeruginosa*: N-butyrylhomoserine lactone (C4-HSL) and N-(3-oxododecanoyl) homoserine lactone (3-oxo-C_{12}-HSL).

mammalian cells. For example, 3-oxo-C_{12}-HSL affects the innate immune response via modulation of the transcriptional activity of the central regulator of gene expression in the innate immune system, NF-κB [16–19]. Furthermore, 3-oxo-C_{12}-HSL has also been demonstrated to induce apoptosis in human breast cancer cells [20], macrophages, and neutrophils [21]. Recently one of us (KDJ) demonstrated that *N*-(3-oxododecanoyl) homoserine lactone performs a previously unrecognized role: the autoinducer itself and the corresponding tetramic acid degradation product (Fig. 2) derived from an unusual Claisen-like condensation reaction, also function as innate bactericidal agents to possibly provide a competitive advantage in mixed species environments [22,23]. The tetramic acid degradation product, 3-(1-hydroxydecylidene)-5-(2-hydroxyethyl) pyrrolidine-2,4-dione (C12-TA), also tightly binds essential metals such as iron, possibly providing a previously unrecognized primordial siderophore.

The competition for iron is particularly intense in the human body, where iron availability is limited by both solubility and host iron storage mechanisms [24,25]. As such, bacterial pathogens depend on siderophores (low molecular weight chelating agents with extraordinarily high affinity for Fe(III)) to obtain iron, and *P. aeruginosa* employs two such molecules: pyochelin and pyoverdin [24,25]. Thus, because of the capacity of C12-TA to bind iron, we hypothesized a role for C12-TA in the iron acquisition of *P. aeruginosa*.

While the tetramic acid ring system has been known since the early 1960s to be a key structural element in various natural products [9] and that the 3-acyl substituted rings provide metal binding capacity, the coordination chemistry of these species has been surprisingly little studied [27–29]. Probably the best studied system is the fungal metabolite, tenuazonic acid where the coordination chemistry with

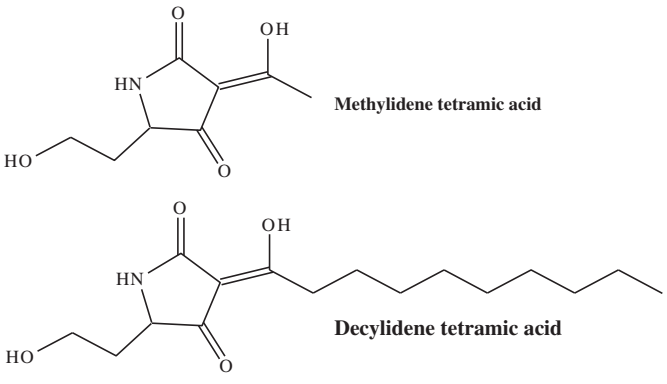

Fig. 2. Structures of methylidene tetramic acid (C4-TA, **1**) and decylidene tetramic acid (C12-TA, **2**), the tetramic acid degradation product of 3-oxo-C_{12}-HSL.

Cu(II), Fe(III), Ni(II) and Mg(II) has been partially explored and a crystal structure of the Cu(II) complex reported [30,31].

Here, using a variety of spectroscopic tools, we describe the coordination chemistry of the decylidene tetramic acid degradation product derived from 3-oxo-C_{12}-HSL, as well as a methylidene analog, with Fe(III) and Ga(III) and discuss their potential biological significance.

2. Materials and methods

2.1. Potentiometric and spectrophotometric titrations

Standard carbonate-free solutions of KOH were prepared from Baker "Dilut-It" ampoules using boiled, purified water (i.e., 18 MΩ resistance; MilliQ) and were stored under Ascarite™ scrubbed argon. Base solutions were standardized with KHP to the phenolpthalein end point. The absence of carbonate (<2%) was confirmed by Gran's plots [32]. Iron solutions were purchased from Fluka ($FeCl_3 \cdot 6H_2O$ in 4% HCl) and the exact iron concentration determined by EDTA titration with Variamine Blue as an indicator. Excess acid in the iron solution was determined by passing an aliquot through a well-washed sample of the acid form of AG 50W-X8 cation exchange resin (Bio-Rad) and titrating the liberated acid. The excess acid was the difference between the total acid and three times the known iron concentration. Spectrophotometric and potentiometric titrations were performed in a jacketed, titration vessel connected to a constant temperature water bath and held at 25.0(1) °C. Ionic strength was fixed at 0.1 M with NaCl. Hydrogen ion concentration was measured using a Mettler-Toledo DL50 titrator connected to a Mettler-Toledo DG111-5C combination electrode which was standardized with a three buffer sequence and corrected (as needed) to read the negative log of the hydrogen ion concentration directly using dilute HCl solutions. Titrant was added to the cell, which was kept under a blanket of Ascarite™ scrubbed argon gas. Ligand protonation constants were determined from the nonlinear refinement of a) the potentiometric titration data using the program PKAS developed by Martell and Motekaitis [33] or b) by NMR titration at 400 MHz in D_2O. For the NMR titrations the pH was adjusted using NaOD (2.0 M) as a titrant and meter readings in D_2O were corrected by adding 0.44 to obtain values of pD [34]. NMR titration data were fitted to a single pK_a equilibrium using SigmaPlot 10.0. Spectrophotometric titration data were analyzed via nonlinear least squares refinement using SigmaPlot 10.0.

2.2. Physical measurements

Routine electrospray-ionization mass spectrometry (ESI-MS) was performed by direct injection on an Agilent LC/MSD Trap XCT Plus mass spectrometer. Isotope distribution patterns were simulated using the program IsoPro. NMR experiments (i.e., ^1H, ^{13}C, DEPT) were run at 30 °C in D_2O containing 0.03% DSS on either a Varian 400 or 600 MHz NMR spectrometer using standard pulse sequences obtained from the VnmrJ™ software (v. 2.2c). UV–visible spectra were recorded using a Cary 50 UV–vis spectrophotometer under PC control using the Cary WinUV software. Cyclic voltammetric experiments were conducted using a BAS (Bioanalytical Systems Inc., West Lafayette, IN) Epsilon voltammetric analyzer. All experiments were done under argon at ambient temperature in solutions with 0.1 M NaCl as the supporting electrolyte. Cyclic voltammograms (CV) were obtained using a three-electrode system consisting of Pt working, platinum wire auxiliary, and SCE reference electrodes. Potentials are reported versus the Ag/AgCl (KCl saturated) couple (197 mV vs NHE). Solution magnetic studies were carried out by the Evans method in Wilmad coaxial NMR tubes at 600 MHz using water as a solvent and t-butyl alcohol as the internal standard.

For Mössbauer spectroscopy solutions were transferred into Delrin® sample holders, frozen in liquid nitrogen, and kept at this

temperature until measurement except for overnight transport on dry ice. The Mössbauer spectra were recorded in the horizontal transmission geometry using a constant acceleration spectrometer operated in conjunction with a 512-channel analyzer in the time-scale mode. The detector consisted of a proportional counter filled with argon–methane (9:1).The source was at room temperature and consisted of 1.4 GBq [^{57}Co] diffused in Rh foil (WissEl, Starnberg, Germany). The spectrometer was calibrated against α-iron at room temperature (RT). For measurements at 77 K, samples were placed in a continuous-flow cryostat (Oxford Instruments). For measurements at 4.3 K and 2 K a helium bath cryostat (MD306, Oxford Instruments) was employed. Spectral data were transferred from the multi-channel analyzer to a PC for further analysis employing the Vinda program on an Excel 2003® platform. Isomer shift δ, quadrupole splitting ΔE_Q, B_{hf} and percentage of the total absorption area were obtained by least-squares fits of Lorentzian lines to the experimental spectra. All values are rounded to last given digit. The isomer shifts (δ), the quadrupole splitting (ΔE_Q), the hyperfine field (B_{hf}) and the line width (Γ) are given in $mm \cdot s^{-1}$. The low relaxation $^6S_{5/2}$ system was simulated with a spin-Hamiltonian [35]. The relative area is given in parts per hundreds.

2.3. Bacterial growth

Utilization of tetramic acid as an iron source was measured with liquid growth assays as follows. Samples were prepared in triplicate in Falcon tubes (50 ml) containing 15 ml M9-glycerol minimal medium (0.5% glycerol): 50 μM of the appropriate complex, 500 μM 2,2-bipyridine, and 0.2% DMSO. The tubes were inoculated to OD_{600} 0.02 with an overnight culture of *P. aeruginosa* PAO6383 (Δ*pvdF*, Δ*pchBA*) grown in M9-glycerol medium. Cultures were incubated at 37 °C with shaking at 250 rpm and OD_{600} was recorded every 24 h for a period of 192 h [36]. Antibiotic activity of the free tetramic acid, and its Ga(III) and Fe(III) analogs were measured against the Gram negative *P. aeruginosa* PAO1 and Gram positive *Staphylococcus aureus* (ATCC25923) in liquid culture containing 100 μM of the appropriate complex and minus the 500 μM 2,2-bipyridine as described above.

C12-TA as an iron source for *P. aeruginosa* was also examined using agar growth assays as follows. Filter disks (6 mm) were sterilized via autoclave, loaded with 10 μl of a solution of C12-TA (500, 250, and 125, and 62.5 μM in methanol) or desferrioxamine (50 μM in water), and the filter disks were allowed to air-dry. M9-soft agar (0.6% agar, 0.5% glycerol) was sterilized via autoclave and, upon cooling to 45 °C, 2,2-bipyridine was added to a final concentration of 500 μM. At this point, an overnight culture of PAO6383 grown in 4 ml LB medium was centrifuged, the cell pellet was washed 3× with M9-glycerol medium and subsequently resuspended in 4 ml M9-glycerol medium. This suspension was used to inoculate the M9-agar, at 45 °C at a dilution of 1:100. The resulting liquid was poured into Petri dishes (15 mL/dish) and allowed to solidify at room temperature. Once the agar solidified, the filter disks were placed on the surface of the agar, and the plates were incubated at 37 °C and growth zones were read after 48 h [37].

3. Results

3.1. Ligands

3-acyl or alkoxycarbonyl substituted tetramic acids such as **1** and **2** are expected to be relatively strong acids, the acidity of which are dependent on the nature of the substituent group [26]. Potentiometric titration of solutions of the C4 analog, **1** and the C12 analog, **2**, involved single proton equilibria and gave estimated of pK_a values of 2.5 and 5.0 respectively. These values were confirmed by NMR titration where plots of chemical shift vs. pH (Fig. 3) could be fitted to single proton equilibria and yielded values of 2.57(3) for **1** and 5.10(3) for **2**.

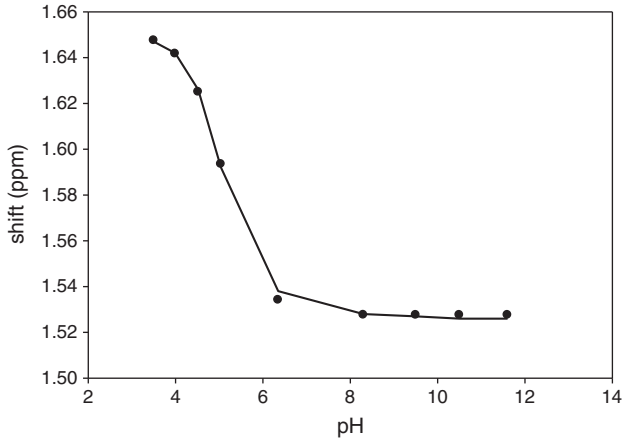

Fig. 3. Plot of chemical shift vs. pH for the NMR titration of 2 at 400 MHz in D_2O. The solid line is a fit of the data to a single pK_a equilibrium using SigmaPlot 10.0.

3.2. Complexation with Fe(III)

Mixing a solution of either **1** or **2** with one of Fe(III) at low pH gives rise to relatively intensely red brown colored solutions reminiscent of those displayed by hydroxamate siderophores [38]. The iron complex of **1** and **2** at pH of 2.5 had a λ_{max} near 450 nm with extinction coefficients between 3500 and 4000 $M^{-1}\,cm^{-1}$. The ca. 4000 $M^{-1}\,cm^{-1}$ extinction coefficients suggest that these spectra arise from O→Fe(III) LMCT transitions. The stoichiometry of the complexes produced at low pH (ca. 2.5) was determined by the method of continuous variations (Fig. 4) and indicated that 3:1 (L:M) complexes were produced as expected for these potentially bidentate ligands. The 3:1 stoichiometry was further supported by ESI-MS analysis. The C4 complex showed the presence of both $Fe(TA)_2^+$ and $Fe(TA)_3$ species when examined at low pH in positive ion mode (Supplementary material). The fraction of the latter species increased with increasing ligand to metal ratio. For the C12 ligand only the $Fe(TA)_3$ species was observed indicative of its more complete formation at this pH.

Optical spectral changes were observed when 80% MeOH/H_2O solutions of the 3:1 complex were raised or lowered in pH indicative of the occurrence of metal complex protonation/deprotonation equilibria. As the pH is lowered from 2.5 to >1.0 the absorbance at ca.

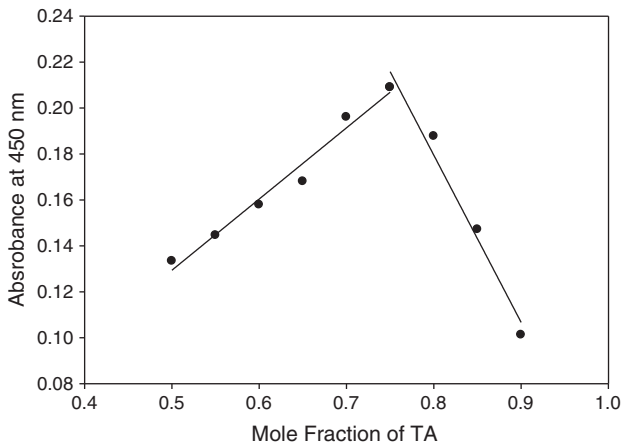

Fig. 4. A Job's method plot of absorbance at 450 nm vs. mole fraction of **1**.

450 nm decreased. In both cases the change in absorbance as a function of pH could be fit to a single proton protonation equilibrium assigned to the reaction:

$$Fe(TA)_3 + H^+ \leftrightarrow Fe(TA)_2^+ + TAH.$$

Increasing the pH range from ca. 2.5 to 9 caused a complete bleaching of the LMCT transition for both the C4 and C12 iron complexes, the pH dependence of which could be fit to a hydrolysis of the tris complex to initially yield a species that we assign to be either a spin coupled (vide infra) μ-dihydroxy or μ-oxobridged dimer or polymer:

$$nFe(TA)_3 + nH_2O \leftrightarrow [Fe_n(TA)_{n+2}(OH)_n] + nTAH$$

or

$$nFe(TA)_3 + n-1H_2O \leftrightarrow [(Fe_2(TA)_2O)_n] + nTAH.$$

Non-linear least squares fits of the combined high and low pH data sets (Fig. 5) gave values for log K_1 and log K_2 of 4.4 and 7.92(10) for the C12 analog and 1.22(2) and 6.3(3) for the C4 complex respectively.

Cyclic voltammetry (Fig. 6) in water at pH 2.5 showed a quasireversible one electron Fe(III) to Fe(II) reduction wave at −352 mv vs. SCE for Fe(**1**)$_3$ and −329 for Fe(**2**)$_3$. Increasing the scan rate from 100 mv/s to 1 V/s or increasing the TA/Fe ratio from 3:1 to 10:1 increased the reversibility of the cyclic voltammogram.

3.3. Mossbauer and magnetic data

For paramagnetic metal ions in general, and Fe(III) in particular, magnetic susceptibility and Mossbauer spectroscopy can yield valuable insights into coordination chemistry. Solution magnetic susceptibility data reveals that at low pH the Fe(TA)$_3$ complexes have the magnetic moment expected for a mononuclear high spin d^5 Fe(III) center with μ = 6.0(2) BM. However as the pH is raised the magnetic moment is seen to fall toward zero (i.e. diamagnetic) in manner paralleling the changes seen in the optical spectra over the same pH regime. We attribute this to the initial formation of a strongly spin coupled dimer (or higher order polymer). More details of this process could be gleaned from Mössbauer spectroscopy.

Samples for Mössbauer spectroscopy were prepared at pH 1.98, 3.05, 4.05, 5.80, 6.07 and 7.48. At 77 K the pH 1.98 sample represents a relaxing $^6S_{5/2}$ system. Comparison with the same sample at 4.3 K discloses temperature dependent spin lattice relaxation due to spin-orbit and orbit-phonon coupling (Fig. 7). However there is still relaxation left at 4.3 K. We attribute this to concentration dependent spin–spin relaxation caused by energy transfer of interacting spins via dipole or exchange coupling. This relaxation accounts for approximately 54% of the absorption area. The spin Hamiltonian simulation yields δ of 0.54 mm·s^{-1}, ΔE_Q of 0.26 mm·s^{-1}, Γ of 0.49 mm·s^{-1}, an almost isotropic hyperfine coupling tensor $A_{xx}/g_N\mu_N$, $A_{yy}/g_N\mu_N$, $A_{zz}/g_N\mu_N$ of −24.0, −24.4, −24.2 T, a zero field splitting D = 22 cm^{-1}, a rhombicity parameter E/D = 0.33 and an asymmetry parameter η of 1. The Mössbauer analysis identifies the low pH sample as a $^6S_{5/2}$ system consistent with the low pH susceptibility data and its formulation as mononuclear Fe(TA)$_3$.

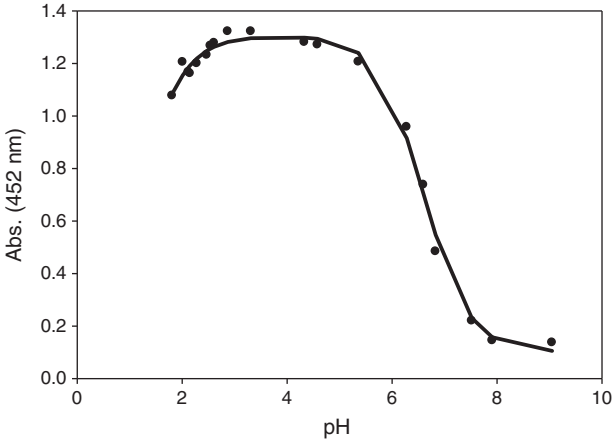

Fig. 5. Spectrophotometric titration of **1** in 80% MeOH/H_2O. The solid line is a fit to the data using a two pK_a model.

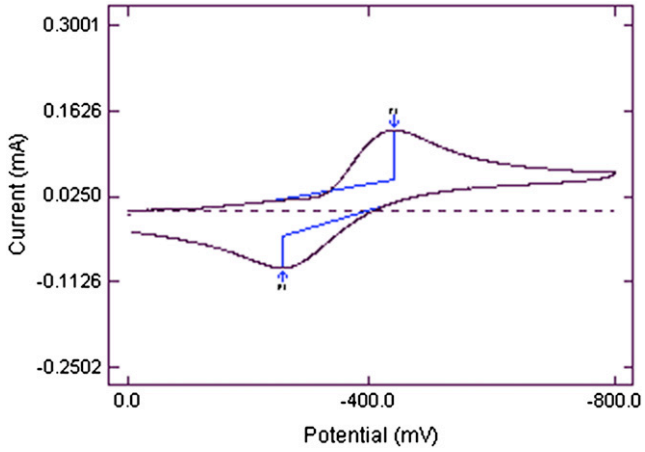

Fig. 6. Cyclic voltammogram (CV) of **1** at 200 mv/s in aqueous solution containing 0.1 M KNO_3 as a supporting electrolyte. Cyclic voltammogram was obtained using a three-electrode system consisting of a Pt disk working, platinum wire auxiliary, and Ag/AgCl reference electrodes. IR compensation was applied before each CV was recorded.

Measurements at 77 K disclose growth of a doublet species with increasing pH in the center of the spectrum. Mössbauer least squares fit analysis reveals, however, that at least two doublet species are present at pH 7.48: component A (δ = 0.45 mm·s^{-1}, ΔE_q = 0.50 mm·s^{-1}, Γ = 0.38 mm·s^{-1}, rel. area 50%) and component B (δ = 0.46 mm·s^{-1}, ΔE_Q = 0.93 mm·s^{-1}, Γ = 0.41 mm·s^{-1}, rel. area 50%). At 4.3 K, the two species split magnetically yielding the following parameters: δ_A = 0.48 mm·s^{-1}, $\Delta E_{Q,A}$ = 0.0 mm·s^{-1}, $B_{HF,A}$ = 49.9 T; δ_B = 0.43 mm·s^{-1}, $\Delta E_{Q,B}$ = 0.0 mm·s^{-1}, $B_{HF,B}$ = 46.4 T. The hyperfine fields observed at 4.3 K reflect the presence of at least two polymeric ferric oxo compounds. Therefore, a simple dimeric species can be excluded at high pH. In the pH range 3.05 through 6.7 the presence of both the polymeric and monomeric ferric iron species displays an equilibrium which is shifted with increasing pH completely into polymeric species.

3.4. Ga(III) complexation and the mode of metal ion coordination

Because of the various tautomeric equilibria (Fig. 8) associated with the TA structure the exact coordination mode of these ligands with iron was in doubt [39]. In solution, NMR would be the probe of choice but it is not amenable to paramagnetic Fe(III) complexes. Thus we have made use of the Ga(III) analogs. Gallium(III) is widely used as a structural probe for Fe(III) since it has approximately the same size and charge but is diamagnetic [21]. ESI-MS confirms that Ga(III) also binds to the tetramic acids with the same 3:1 stoichiometry as Fe(III) (i.e., m/z of 622 and 624 amu for the C4 and 958 and 960 amu for the C12 the 3:2 ratio reflecting the relative abundance of ^{69}Ga and ^{71}Ga (Fig. 9)). The ^{13}C NMR spectra of the Ga(III) complex of the C4 ligand display a number of changes with respect to the free ligand. Most revealing are the ca. 1.8–5.6 ppm coordination induced shifts (CIS) in the resonances for carbons 2, 3, 6 and 7 (Table 1) as compared to values of 0.2 ppm or less for the remaining carbons. The magnitude of the shifts for the proposed coordinating groups is

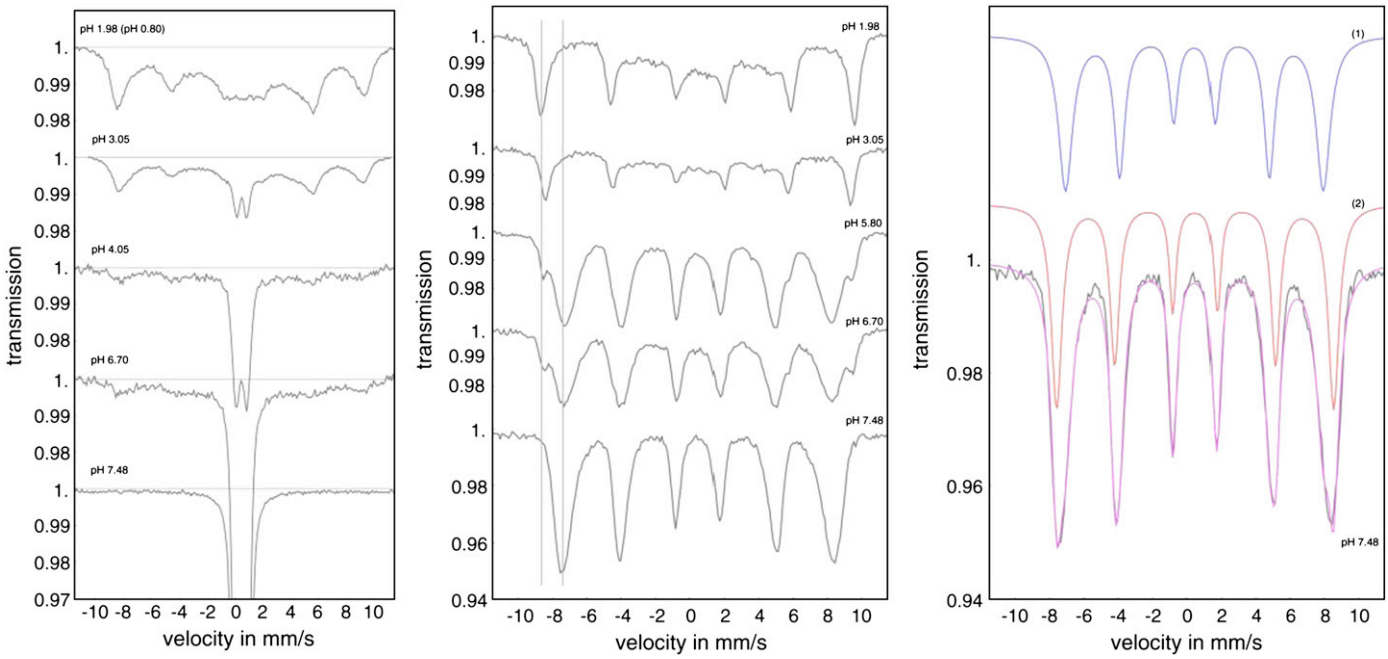

Fig. 7. Comparison of Mössbauer spectra of **1** as a function of pH: left panel) 4.3 K, center panel) 77 K, and right panel) calculated subspectra and composite experimental spectrum at pH of 7.48.

similar to those seen with other ligands such as siderophores [40,41] and indicates unequivocally that the ligand is bound to Ga(III) as shown in Fig. 8a and inferentially the same for Fe(III).

3.5. Biological effects

With the interactions between TA and Fe(III) clearly delineated, a role for C12-TA in the iron acquisition of *P. aeruginosa* was envisaged. Toward this end, we examined the capacity of C12-TA to facilitate the growth of the siderophore-mutant *P. aeruginosa* strain PAO6383 (Δ*pvdF*, Δ*pchBA*) under iron limiting conditions [36]. PAO6383 was grown in both M9-glycerol medium and agar containing 500 μM 2,2′-bipyridine to create iron-deficient conditions. In the case of the liquid culture experiments, M9-glycerol medium was supplemented with 50 μM C12-TA, which did not exhibit significant growth restoration of PAO6383 after 6 days (data not shown). In a separate set of experiments, PAO6383 was grown on 0.6% agar plates containing 500 μM 2,2′-bipyridine. Filter disks containing between 500 and 62.5 μM C12-TA, as well as 50 μM desferrioxamine mesylate salt, were placed on the agar. In this case, only desferrioxamine, a fungal siderophore that may be used by *P. aeruginosa* [42], was able to promote the growth of PAO6383. As such, these data indicate that C12-TA alone is not sufficient to provide *P. aeruginosa* with the iron required for growth.

We also verified that the free C12-TA but not its C4 analog display bacteriostatic activity against the Gram positive organism *S. aureus*. Since Ga(III) complexes of some siderophores have been reported to have potent antibacterial activity [41], the possibility that the Ga(III) complex would show enhanced activity was also investigated. However examination of the activity of the Fe(III) and Ga(III) complexes against *S. aureus* showed little if any toxicity beyond that of the free tetramic acid, suggesting that metal complexation had no role to play in the bacteriostatic effect.

4. Discussion

Although tetramic acids are expected to be relatively strong acids, the two ligands we examined in detail (**1** and **2**) differ considerably in their relative acidity. The significantly greater acidity of **1** vs. **2** is likely the result of two factors, both of which arise from the extended alkyl chain of **2**. For one, the addition of weakly electron-donating methylene groups serves to destabilize the anionic species and increase the pK_a of **2**. A more significant contribution likely arises from the hydrophobic nature of **2**, which contributes to the increased pK_a through the decreased solvation of the deprotonated species [43,44].

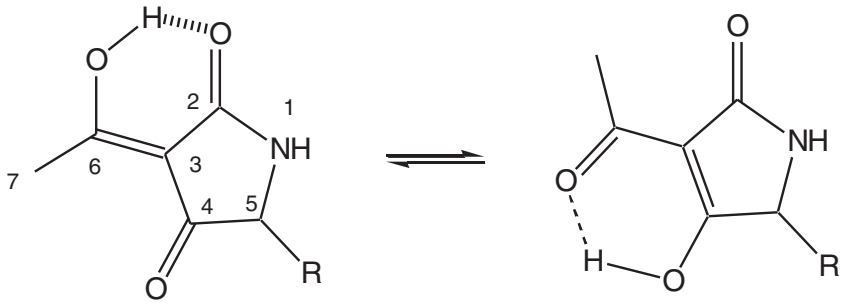

Fig. 8. Tautomeric equilibria in tetramic acids.

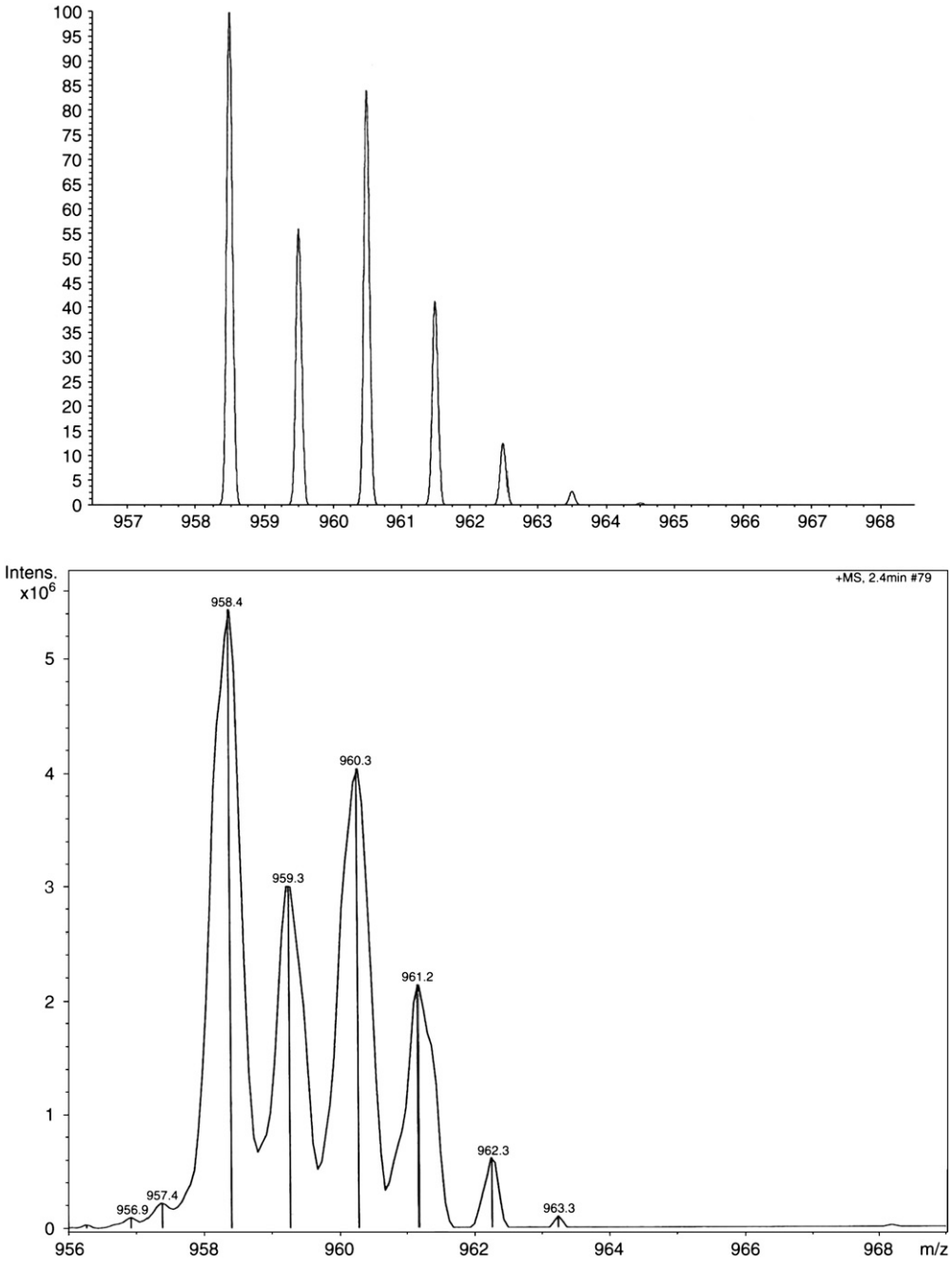

Fig. 9. Positive ion mode ESI-MS of the Ga(III) complex of **2**. Upper) calculated isotope distribution pattern for $Ga(2)_3$, lower) experimental isotope pattern, positive ion ESI-MS.

A final reasoning for this observation may be the result of aggregation and molecular association of the C12-TA in solution. Recent studies have demonstrated that fatty acids, which possess the structural characteristic aliphatic chain connected to an acidic head group similar to C12-TA, exhibit increased pK_a values when the carbon tail extends past C_6. This observation is a result of the tighter intermolecular interactions via van der Waals forces, resulting in a closer proximity of both protonated and deprotonated species. As a result, the deprotonated species serve to stabilize the acid proton and increase the pK_a of the solution [45,46]. Because of the structural similarities of C12-TA to fatty acids, this phenomenon likely contributes to the significant differences in pK_a between C4- and C12-TA.

Table 1
Coordination inducted shifts in the ^{13}C NMR spectra of **1**. Numbering is according to Fig. 8.

C #	CIS (ppm)
2	+1.9
3	−1.8
4	−0.3
5	+0.14
6	+5.6
7	+3.6
8	−0.1
9	+0.86

As originally reported the tetramic acids produced as degradation products from QS HSL do indeed bind Fe(III) with appreciable affinity (table 2). However Table 2 illustrates a number of important points. The first is that while the overall formation constants for Fe(III) complexation appear to be similar to those of known siderophores such as DFO and pyoverdin, because of the differing denticity and acidity of the ligands, they are not nearly as effective iron chelators at

Table 2
Fe(III) binding constants for **1**, **2** and related ligands.

Compound	Log β[a]	pM_1	pM_2	pM_3	Ref
3-acetyl tetramic acid	28.6	19.6	25.6	19.6	28
3-acetyl-5-methyl tetramic acid	26.3	17.3	23.3	17.3	28
Acetohydroxamic acid	28.3	12.5			47
1	nd	17.3[b]			This work
2	28.8	19.8	25.8	19.8	22
Pyoverdin	30.8	27.0			22
Ferrioxamine B	30.6	26.6	28.6	30.0	47

pM_1: $[Fe^{3+}]_{tot} = 1\ \mu M$, $[L]_{tot} = 10\ \mu M$, pH = 7.4.
pM_2: $[Fe^{3+}]_{tot} = 1\ \mu M$, $[L]_{tot} = 1\ mM$, pH = 7.4.
pM_3: $[Fe^{3+}]_{tot} = 1\ \mu M$, $[L]_{tot} = 10\ \mu M$, pH = 9.0.
[a] β_{130} for compounds 1–5 and β_{110} for 6 and 7.
[b] Estimate based on reported binding constant of the closely related 3-acetyl-5-methyltetramic acid. Precipitation of $Fe(OH)_3$ will occur if the pM value is less than 16 at pH 7.4 and 21 at pH 9.0.

physiological pH, as indicated by their pM values. Secondly, since these tetramic acids are relatively strong acids, particularly as compared as compared to the very weakly acidic behavior of most of the iron binding moieties prevalent in the siderophores, they do not suffer strong competition from protons making them relatively more effective at low pH than some siderophores. However, correspondingly, because of relatively facile hydrolysis they compete rather poorly with hydroxide ion and indeed at higher pH are expected (and observed) to be unstable with respect to precipitation of $Fe(OH)_3$. Finally, three of these bidentate ligands are needed to satisfy the octahedral six coordinate structure preferred by Fe(III) as compared to a single, typically hexadentate, siderophore molecule. This leads to a third power dependence on iron binding with respect to ligand concentration for the former and thus they are only effective iron chelators at relatively high concentrations.

While these ligands can bind iron well under certain conditions it is important to note that the species present at near neutral and biologically relevant pH does not appear to be exclusively the expected $Fe(TA)_3$ complex. Indeed in the case of the C4 ligand **1** only about 7% of the total iron is expected to be present as $Fe(TA)_3$ at pH 7.4 while for the C12 ligand the tris complex represents approximately 75% of the total. The other species we formulate as unstable μ-dihydroxy or μ-oxobridged dimeric or higher order polymeric species which ultimately yield solid $Fe(OH)_3$. It is further worth noting that for many similar ligands there is often a correlation between the LMCT band maximum or pM values with redox potential. The measured values of −352 and −329 mv for the iron complexes of **1** and **2** are within those expected based upon such previously published correlations [47]. These modestly low redox potentials also lie well within the range accessible to biological reductants and thus iron bound to these complexes could be readily released by a reductive type mechanism. However in total, the data presented here argues against any overt iron transport role for these molecules.

If iron transport is not the major biological role for these molecules, then what is? It has been demonstrated that iron serves as a signal for biofilm formation [48] and is required for swarming in *P. aeruginosa* [49,50]. Given the link between these behaviors and quorum sensing, [5,7] coupled with the iron affinity of C12-TA and the fact that it is derived from a major autoinducer of *P. aeruginosa*, several plausible biological functions of C12-TA may be postulated. We have initiated studies to decipher the role of C12-TA in these processes, but a clear role for C12-TA has yet to be definitively assigned. Additionally, *P. aeruginosa* has been demonstrated to lyse *S. aureus* and gain access to its intracellular iron pools [51]. While C12-TA does not directly promote the growth of *P. aeruginosa*, it may also play a role in this process as C12-TA has been recently reported as an antibacterial that targets the membrane of *S. aureus* [23]. Thus, in light of the myriad roles of iron in the survival and pathogenesis of *P. aeruginosa*, the distinct biological function of TA-Fe complexes remains unresolved and is a subject of ongoing investigation in our laboratories.

Supplementary data to this article can be found online at doi:10.1016/j.jinorgbio.2011.10.009.

Acknowledgments

The work of LHB and BFM was in part supported by DFG grant Ma916/20-1 and that of CJC by NOAA grants #NA04OAR4170038 and NA08OAR4170669, California Sea Grant College Program Project numbers R/CZ-198 and R/CONT-205 and NSF grant CHE-0924313. ANR was supported at SDSU by National Institutes of Health, MBRS grant #2R25GM058906 and TH by a DAAD RISE fellowship. CAL, AKS, and KDJ were supported by National Institutes of Health, AI077644. We also thank Cornelia Reimmann for providing PAO6383.

References

[1] T.R. De Kievit, B.H. Iglewski, Bacterial quorum sensing in pathogenic relationships, Infect. Immun. 68 (2000) 4839–4849.
[2] C.M. Waters, B.L. Bassler, Quorum sensing: cell-to-cell communication in bacteria, Annu. Rev. Cell Dev. Biol. 21 (2005) 319–346.
[3] C. Fuqua, E.P. Greenberg, Listening in on bacteria: acyl-homoserine lactone signalling, Nat. Rev. Mol. Cell Biol. 3 (2002) 685–695.
[4] G.J. Lyon, R.P. Novick, Peptide signaling in *Staphylococcus aureus* and other Gram-positive bacteria, Peptides 25 (2004) 1389–1403.
[5] D.G. Davies, M.R. Parsek, J.P. Pearson, B.H. Iglewski, J.W. Costerton, E.P. Greenberg, The involvement of cell-to-cell signals in the development of a bacterial biofilm, Science 280 (1998) 295–298.
[6] H.B. Tang, E. DiMango, R. Bryan, M. Gambello, B.H. Iglewski, J.B. Goldberg, A. Prince, Contribution of specific *Pseudomonas aeruginosa* virulence factors to pathogenesis of pneumonia in a neonatal mouse model of infection, Infect. Immun. 64 (1996) 37–43.
[7] T. Kohler, L.K. Curty, F. Barja, C. van Delden, J.C. Pechere, Swarming of *Pseudomonas aeruginosa* is dependent on cell-to-cell signaling and requires flagella and pili, J. Bacteriol. 182 (2000) 5990–5996.
[8] R.S. Smith, B.H. Iglewski, *Pseudomonas aeruginosa* quorum sensing as a potential antimicrobial target, J. Clin. Invest. 112 (2003) 1460–1465.
[9] M.G. Page, J. Heim, Prospects for the next anti-Pseudomonas drug, Curr. Opin. Pharmacol. 9 (2009) 558–565.
[10] V.E. Wagner, B.H. Iglewski, *P. aeruginosa* biofilms in CF infection, Clin. Rev. Allergy Immunol. 35 (2008) 124–134.
[11] C. Winstanley, J.L. Fothergill, The role of quorum sensing in chronic cystic fibrosis *Pseudomonas aeruginosa* infections, FEMS Microbiol. Lett. 290 (2009) 1–9.
[12] J.W. Bendig, P.W. Kyle, P.L. Giangrande, D.M. Samson, B.S. Azadian, Two neutropenic patients with multiple resistant *Pseudomonas aeruginosa* septicaemia treated with ciprofloxacin, J. R. Soc. Med. 80 (1987) 316–317.
[13] F. Franzetti, M. Cernuschi, R. Esposito, M. Moroni, Pseudomonas infections in patients with AIDS and AIDS-related complex, J. Intern. Med. 231 (1992) 437–443.
[14] J.B. Lyczak, C.L. Cannon, G.B. Pier, Establishment of *Pseudomonas aeruginosa* infection: lessons from a versatile opportunist, Microbes and infection / Institut Pasteur 2 (2000) 1051–1060.
[15] E.B. Breidenstein, C. de la Fuente-Nunez, R.E. Hancock., *Pseudomonas aeruginosa*: all roads lead to resistance, Trends Microbiol. 19 (2011) 419–426.
[16] A. Jahoor, R. Patel, A. Bryan, C. Do, J. Krier, C. Watters, W. Wahli, G. Li, S.C. Williams, K.P. Rumbaugh, Peroxisome proliferator-activated receptors mediate host cell proinflammatory responses to *Pseudomonas aeruginosa* autoinducer, J. Bacteriol. 190 (2008) 4408–4415.
[17] V.V. Kravchenko, G.F. Kaufmann, J.C. Mathison, D.A. Scott, A.Z. Katz, D.C. Grauer, M. Lehmann, M.M. Meijler, K.D. Janda, R.J. Ulevitch, Modulation of gene expression via disruption of NF-kappaB signaling by a bacterial small molecule, Science 321 (2008) 259–263.
[18] V.V. Kravchenko, G.F. Kaufmann, J.C. Mathison, D.A. Scott, A.Z. Katz, M.R. Wood, A.P. Brogan, M. Lehmann, J.M. Mee, K. Iwata, Q. Pan, C. Fearns, U.G. Knaus, M.M. Meijler, K.D. Janda, R.J. Ulevitch, N-(3-oxo-acyl)homoserine lactones signal cell activation through a mechanism distinct from the canonical pathogen-associated molecular pattern recognition receptor pathways, J. Biol. Chem. 281 (2006) 28822–28830.
[19] K.P. Rumbaugh, J.A. Colmer, J.A. Griswold, A.N. Hamood, The effects of infection of thermal injury by *Pseudomonas aeruginosa* PAO1 on the murine cytokine response, Cytokine 16 (2001) 160–168.
[20] L. Li, D. Hooi, S.R. Chhabra, D. Pritchard, P.E. Shaw, Bacterial N-acylhomoserine lactone-induced apoptosis in breast carcinoma cells correlated with down-modulation of STAT3, Oncogene 23 (2004) 4894–4902.
[21] K. Tateda, Y. Ishii, M. Horikawa, T. Matsumoto, S. Miyairi, J.C. Pechere, T.J. Standiford, M. Ishiguro, K. Yamaguchi, The *Pseudomonas aeruginosa* autoinducer N-3-oxododecanoyl homoserine lactone accelerates apoptosis in macrophages and neutrophils, Infect. Immun. 71 (2003) 5785–5793.
[22] G.F. Kaufmann, R. Sartorio, S.H. Lee, C.J. Rogers, M.M. Meijler, J.A. Moss, B. Clapham, A.P. Brogan, T.J. Dickerson, K.D. Janda, Revisiting quorum sensing: discovery of

additional chemical and biological functions for 3-oxo-N-acylhomoserine lactones, Proc. Natl. Acad. Sci. U. S. A. 102 (2005) 309–314.
[23] C.A. Lowery, J. Park, C. Gloeckner, M.M. Meijler, R.S. Mueller, H.I. Boshoff, R.L. Ulrich, C.E. Barry III, D.H. Bartlett, V.V. Kravchenko, G.F. Kaufmann, K.D. Janda, Defining the mode of action of tetramic acid antibacterials derived from *Pseudomonas aeruginosa* quorum sensing signals, J. Am. Chem. Soc. 131 (2009) 14473–14479.
[24] S.C. Andrews, A.K. Robinson, F. Rodriguez-Quinones, Bacterial iron homeostasis, FEMS Microbiol. Rev. 27 (2003) 215–237.
[25] C. Ratledge, L.G. Dover, Iron metabolism in pathogenic bacteria, Annu. Rev. Microbiol. 54 (2000) 881–941.
[26] B.J.L. Royles, Naturally occurring tetramic acids: structure, isolation, and synthesis, Chem. Rev. 95 (1995) 1981–2001.
[27] G. Athanasellis, O. Igglessi-Markopoulou, J. Markopoulou, Tetramic and tetronic acids as scaffolds in bioinorganic and bioorganic chemistry, Bioinorganic Chemistry and Applications 2010 (2010) 1–11.
[28] W.O. Foye, J.R. Lo., Metal-binding abilities of antibacterial heterocyclic thiones, J. Pharm. Sci. 61 (1972) 1209–1212.
[29] M.H. LeBrun, L. Nicolas, M. Boutar, F. Gaudemer, S. Ranomenjanahary, A. Gaudemer, Relationships between the structure and the phytotoxicity of the fungal toxin tenuazonic acid, Phytochem. 27 (1988) 77–84.
[30] M.H. Lebrun, P. Duvert, F. Gaudemer, A. Gaudemer, C. Deballon, P. Boucly, Complexation of the fungal metabolite tenuazonic acids with copper (II), iron (III), nickel (II) and magnesium (II) ions, J. Inorg. Biochem. 24 (1985) 167–181.
[31] A. Dippenaar, C.W. Holzapfel, J.C.A. Boeyens, Crystal structure of copper bis (tenuazonate) monohydrate, J. Crystr. Mol. Struct. 7 (1977) 189–197.
[32] G. Gran, Analyst 77 (1952) 661–670.
[33] A.E. Martell, R.J. Motekaitis, The Determination and Use of Stability Constants, Wiley-VCH Inc., New York, 1992.
[34] D.D. Perrin, B. Dempsey, Buffers for pH and Metal Ion Control, Chapman and Hall, London, 1974.
[35] Gunnlaugsson, H. P.: Vinda, plugin for the Microsoft Excel program, designed for the analysis of Mössbauer Spectra. http://users-phys.au.dk/hpg/vinda.htm.
[36] L. Michel, A. Bachelard, C. Reimmann, Ferripyochelin uptake genes are involved in pyochelin-mediated signalling in *Pseudomonas aeruginosa*, Microbiology 153 (2007) 1508–1518.
[37] W. Rabsch, G. Winkelmann, The specificity of bacterial siderophore receptors probed by bioassays, Biol. Met. 4 (1991) 244–250.
[38] W.R. Harris, C.J. Carrano, K.N. Raymond, Coordination chemistry of microbial iron transport compounds. 16. Isolation, characterization, and formation constants of ferric aerobactin, J. Am. Chem. Soc. 101 (1979) 2722–2727.
[39] M.J. Nolte, P.S. Steyn, P.L. Wessels., Structural investigations of 3-acylpyrrolidine-2,4-diones by nuclear magnetic resonance spectroscopy and X-ray crystallography, J.C.S. Perkin I (1980) 1057–1065.
[40] G. Zhang, S.A. Amin, F.C. Küpper, P.D. Holt, C.J. Carrano, A. Butler, Ferric stability constants of representative marine siderophores: marinobactins, aquachelins, and petrobactin, Inorg. Chem. 48 (2009) 11466–11473.
[41] C.J. Carrano, H. Drechsel, D. Kaiser, G. Jung, B. Matzanke, G. Winkelmann, N. Rochel, A.M. AlbrechtGary, Coordination chemistry of the carboxylate type siderophore rhizoferrin: the iron(III) complex and its metal analogs, Inorg. Chem. 35 (1996) 6429–6436.
[42] M.A. Llamas, M. Sparrius, R. Kloet, C.R. Jimenez, C. Vandenbroucke-Grauls, W. Bitter, The heterologous siderophores ferrioxamine B and ferrichrome activate signaling pathways in *Pseudomonas aeruginosa*, J. Bacteriol. 188 (2006) 1882–1891.
[43] K. Bowden, R.C. Young., Transmission of polar effects.11. Polar and steric effects in reactions of arylaliphatic carboxylic acids, Can J Chemistry 47 (1969) 2775.
[44] A.D. Headley, M.E. Mcmurry, S.D. Starnes, Effects of substituents on the acidity of acetic-acids, J. Org. Chem. 59 (1994) 1863–1866.
[45] J.R. Kanicky, A.F. Poniatowski, N.R. Mehta, D.O. Shah, Cooperativity among molecules at interfaces in relation to various technological processes: effect of chain length on the pK(a) of fatty acid salt solutions, Langmuir 16 (2000) 172–177.
[46] J.R. Kanicky, D.O. Shah, Effect of premicellar aggregation on the pK(a) of fatty acid soap solutions, Langmuir 19 (2003) 2034–2038.
[47] A.L. Crumbliss, J.M. Harrington, Iron sequestration by small molecules: thermodynamic and kinetic studies of natural siderophores and synthetic model compounds, Adv. Inorg. Chem. 61 (2009) 179–250.
[48] P.K. Singh, M.R. Parsek, E.P. Greenberg, M.J. Welsh, A component of innate immunity prevents bacterial biofilm development, Nature 417 (2002) 552–555.
[49] E. Deziel, F. Lepine, S. Milot, R. Villemur, rhlA is required for the production of a novel biosurfactant promoting swarming motility in *Pseudomonas aeruginosa*: 3-(3-hydroxyalkanoyloxy)alkanoic acids (HAAs), the precursors of rhamnolipids, Microbiology 149 (2003) 2005–2013.
[50] P. Nadal Jimenez, G. Koch, E. Papaioannou, M. Wahjudi, J. Krzeslak, T. Coenye, R.H. Cool, W.J. Quax, Role of PvdQ in *Pseudomonas aeruginosa* virulence under iron-limiting conditions, Microbiology 156 (2010) 49–59.
[51] L.M. Mashburn, A.M. Jett, D.R. Akins, M. Whiteley, *Staphylococcus aureus* serves as an iron source for *Pseudomonas aeruginosa* during in vivo coculture, J. Bacteriol. 187 (2005) 554–566.